Anti-cancer Effects and Mechanisms of Diosmin in HepG2 Cells in Vitro Revealed by Network Pharmacology and Molecular Docking

Cuilin Cheng (ccuilin@hit.edu.cn)
Harbin Institute of Technology https://orcid.org/0000-0002-5880-1412
Rongchun Wang
Harbin Institute of Industry: Harbin Institute of Technology https://orcid.org/0000-0002-3747-7553
Debin Xia
Harbin Institute of Industry: Harbin Institute of Technology
Yingchun Zhang
Harbin Institute of Industry: Harbin Institute of Technology
Ning Xu
Harbin Institute of Industry: Harbin Institute of Technology
Weihong Lu
Harbin Institute of Industry: Harbin Institute of Technology
Zhiqiang Zheng
Academy of Military Sciences of the Chinese Peoples Liberation Army Graduate School: Academy of Military Sciences of the Chinese Peoples Liberation Army Graduate Department

Research Article

Keywords: Diosmin, Anti-cancer, Network pharmacology, Molecular docking, Action mechanism

Posted Date: October 25th, 2021

DOI: https://doi.org/10.21203/rs.3.rs-968920/v1

Abstract

Diosmin is able to exert anti-cancer effects on various cancer cells, including Caco-2 and HT-29. Herein, we set out to investigate the anti-cancer effects and action mechanisms of diosmin in the HepG2 cell line. We utilized the PharMapper server and Genecards database to identify the target proteins. The Autodock software was used to dock key targets with diosmin to identify action sites. MTT and Western blot assays were utilized to determine cancer cell proliferation, as well as expression of related target proteins in order to validate the antitumor effect of diosmin. Results demonstrated that 13 key targets and 14 tumor signaling pathways were involved in the anti-cancer effect of diosmin. *In vitro* experiments demonstrate that the number of HepG2 cells were significantly reduced with increasing Bax/Bcl-2 expression ratio after 200 μg/mL of diosmin treatment. Concomitantly, the degrees of RAS p-ERK and p-MEK were significantly decreased, whereas those of Caspase-3 was increased. In conclusion, antitumor effect of diosmin is a comprehensive effect of multi-cell signaling pathways, multi-biological processes and multiple targets. The MAPK signaling pathway is one important pathways by which diosmin exerts its anti-tumor effects. The study provides a rationale for the application of diosmin in the treatment of HepG2.

1. Introduction

Hepatocellular carcinoma (HCC), the most common of the primary liver cancers, is the fifth most common malignancy in the world, as well as the second most frequent cause of cancer-related deaths worldwide [1, 2]. In China, HCC morbidity and mortality contribute to approximately 50% of total number of cases of liver cancer, as well as liver cancer-related deaths [3]. Chemotherapy and surgery are effective methods for treatment of cancer [4, 5]. Unfortunately, the lack of effective and targeted drugs has led to a low five-year survival rate. One exception is sorafenib, a tyrosine protein kinase inhibitor [6]. In addition, chemotherapy is often accompanied with serious side effects, including immunodeficiency, cell damage, and neurological, renal, and cardiac toxicity. Over the past 10 years, the global incidence of liver cancer has not been effectively controlled [7]. Therefore, it is necessary to identify and develop natural anti-cancer drugs with good anti-tumor activity, as well as low side effects [8].

Flavonoids, which are plant-derived ubiquitous components of the human diet, are thought to be promising candidates for the prevention and treatment of cancer [9, 10]. They are low molecular weight compounds that are comprised of a three-ring structure with various substitutions [11]. Flavonoids possess anti-tumor activity against various human cancer cell lines and xenograft systems of human tumors, which suggests the presence of potential anti-cancer agents [12].

Diosmin, a flavonoid, was initially isolated from *Scrophularia nodosa* in 1925, and then utilized as a medicine for venous lymphatic insufficiency in 1969. Since then, scientists have carried out extensive research on its function. In addition, these results indicate that diosmin can be used for the treatment of hemorrhoids, lymphedema and varicose veins [13]. It has also been reported that diosmin exhibits anti-cancer, antimicrobial, antioxidant, oestrogenic and anti-inflammatory activities [14]. We have discovered

that diosmin has the opposite effect, such as antiproliferative and pro-apoptotic activity, on tumor cells. This includes oral cancer cells, colon cancer cells, breast cancer cells and liver cancer cells [15, 16, 17].

Nevertheless, the antitumor mechanism of diosmin remains unknown. In addition, research on proliferation inhibition of diosmin in HepG2 cells has rarely been reported. Network pharmacology and molecular docking technology are emerging and promising techniques in pharmacological research over recent years [18]. Molecular docking has been applied to evaluate the relationship between small molecule compound ligands and macromolecular bioreceptors via molecular mechanics energy analysis. It has been widely used in virtual screening of target proteins, and elucidating the mechanisms of action. The credibility of the results has been validated among various molecular pharmacological experiments [19].

Herein, we analyzed and identified potential target proteins of diosmin from the PharmMapper and Genecards database, the string database and Gene Ontology Resource. Moreover, we identified the main tumor suppressor pathway of diosmin using KEGG analysis. Furthermore, we performed molecular docking analysis to determine the site of action of the main target proteins, using the small molecule diosmin as substrate. Finally, western blot technology was utilized to determine the function of diosmin in inhibiting proliferation of HepG2 cells. These results provide a scientific theoretical basis for the development of anti-cancer drugs through the use of diosmin as the lead or analogue. Fig. 1 depicts the flowchart of our study.

2. Material And Methods

2.1. Chemicals

The DNA content quantitation measurement kit, 3-(4,5-Dimethylthiazol-2-yl)-2,5-diphenyltetrazolium bromide (MTT) were purchased from Solarbio Science & Technology Co., Ltd. (Beijing, China). The BCA protein assay kit was purchased from by Beyotime Biotechnology (Shanghai, China). The chemicals that were required for cell culture, including RPMI 1640 medium, heat-inactivated fetal bovine serum (FBS) and trypsin were bought from Hyclone Co., USA. Antibodies that targeted ERK, p-ERK, MEK, p-MEK, HRAS, Raf-1, Bax, Bcl-2, Caspase-3 and β-actin were purchased from Wanleibio Co. (Shenyang, China). Other chemicals were of analytical grade and purchased from local suppliers.

2.2. Screening the tumor suppressor pathway of diosmin by network pharmacology

2.2.1. Screening of Diosmin's action targets

The chemical structure of diosmin was obtained via a Traditional Chinese Medicine System Pharmacology Database and Analysis Platform (TCMSP). The molecular structure of diosmin was saved in a mol2 format. The molecular structure of diosmin was imported into the PharmMapper database,

setting human protein targets only. Results were merged from database and duplicated targets were deleted to predict the potential targets of diosmin.

2.2.2. Screening of anti-cancer targets

To identify the potential targets for the anti-cancer effect of diosmin, we selected the Genecards database, entered cancer, anti-cancer, tumor and anti-tumor, searched for existing cancer-related genes, integrated the data, and deleted the duplicate genes.

2.2.3. Diosmin-anti-cancer target network structure

Next, we entered the intersection target into the String database, limited the species to only human, and obtained the interaction between the target proteins that have potential anti-cancer effect of diosmin. The information obtained was then imported into the Cytoscape software (version 3.6.1) to construct a protein-coded interaction network. Within this network, a node represents a protein, and the degree value indicates the number of other nodes that are directly connected to the node. The larger the degree, the more important the node is within the network. Closeness centrality is reciprocal of the average geodesic distance between the node to additional nodes. Furthermore, it reflects the degree in the central position of this node within the network structure. As the betweenness centrality depicts the position of the node between two other nodes that do not have direct connectivity between them, it can affect these other two nodes. Therefore, betweenness centrality is an indicator that reflects the importance of the node, and namely the importance of protein. According to the degree value and betweenness centrality, the important proteins were selected. Then, we utilized the Disgenet database [20] in order to obtain information on the potential anti-cancer effect of diosmin.

2.2.4. KEGG pathway analysis

The biological information annotation Database for Annotation, Visualization and Integrated Discovery (DAVID) functions to integrate biological data and analysis tools in order to provide a systematic and comprehensive biological function annotation information for both large-scale gene and protein lists. The anti-cancer targets of diosmin were then chosen to identify biological processes and pathways that were involved using the DAVID database for Gene Ontology (GO) analysis. We performed Kyoto Encyclopedia of Genes and Genomes (KEGG) pathway enrichment analysis for the differential target genes and drew a diagram of the anti-cancer pathway of diosmin.

2.3. Determination of the binding site between diosmin and target protein

We performed the docking study using AutoDock in order to find a possible binding mode and the affinity power between diosmin and the target protein. The binding energy between diosmin and the protein was evaluated to select the main target protein and diosmin molecules in order to evaluate binding activity.

2.4. The anti-tumor pathway of diosmin on HepG2

2.4.1. Cell Culture

The human hepatoma HepG2 cell line was acquired from the Cell Bank of the Chinese Academy of Sciences (Shanghai, China) and cultured in RPMI 1640 medium (Hyclone) supplemented with 10% (v/v) heat-inactivated FBS. Cells were incubated at 37°C in a humidified atmosphere of 95% air and 5% CO_2 until they reached confluence [21]. Typically, cells were passaged using trypsin and maintained in RPMI 1640 medium.

2.4.2. Cell proliferation assay

The MTT assay is a colorimetric method to evaluate survival and cell proliferation. Succinate dehydrogenase in living cells was able to deoxygenate exogenous MTT into a water-insoluble, blue-violet formazan and deposit it into cells. Next, we utilized this assay to screen for the pharmacodynamic effects of diosmin on multiple human cancer cell lines [21, 22].

HepG2 cells were incubated into 96-well culture plates at a density of 1×10^4 cells in each well. The cells were then treated with 0, 50, 100, 150, 200, 250, 300, 350, and 400 μg/mL diosmin while the control groups were treated with phosphate buffer saline (PBS). After 24 hours, the supernatant was removed and 100 uL of culture medium was added. Next, 20 uL of MTT (5 mg/mL) was added to each well and under the same conditions, incubated for 4 h. The supernatant was then discarded, and a 150 uL dimethyl sulfoxide (DMSO) was added for 10 min in order to dissolve the converted violet dye into a 96-well plate. The absorbance was quantified through the use of an automatic microplate-reader with 490 nm wavelength. Cell viability was then expressed as a ratio of optical densities of the treatment group to normal group, and calculated according to the following formula:

$$\text{Cellviability}(\%) = \frac{OD_{treatment} - OD_{blank}}{OD_{normal} - OD_{blank}} \times 100\% \quad (1)$$

2.4.3. Cell morphology analysis

The morphological changes of HepG2 cells were directly observed using an inverted microscope and further analyzed using HE staining. Use of HE staining causes the cytoplasm to be stained red and the nucleus to be stained blue. Changes of cell structure influence the light-shielding rate, and the stained cell images appear under a light microscope. HepG2 cells treated with diosmin were collected after trypsinization, and then incubated at a density of 1×10^5/mL on a coverslip, which was placed into a 6-well plate. After corresponding time, the coverslip was taken out. Then, the cell samples were fixed with 95% ethanol for 20 min, followed by HE staining and observation under a light microscope.

2.4.4. Colony formation assay

In brief, we seeded HepG2 cells in a 6 well-plate (400 cells per well), which was cultured in a humidified incubator at 37°C and 5% CO_2. After 24 hours, the medium was replaced with RPMI 1640 supplemented with the final concentration of 200 μg/mL diosmin. The culture medium was refreshed every 48 h for the next 14 days. The medium was then removed and 1 mL of methanol per well was added to fix the cells.

10 minutes later, the colonies were stained with crystal violet. Then, distilled water was utilized to slowly wash away the excess dye solution, and the colonies were observed under a light microscope (Photoelectric Instrument Co. Ltd, Chongqing, China).

2.4.5. Western blot for protein expression detection

Cells were plated into 6-well plates at a density of 1.0×10^6 cells per well. After adhering, cells were treated with diosmin for 24 hours. Proteins were then extracted from the treated and untreated cells, and the concentration was determined using the BCA protein assay kit. Protein samples were separated via a 12% sodium dodecyl sulfate-polyacrylamide electrophoresis, and then transferred to 0.22 μm NC membranes. The membranes were then blocked with 5% skimmed milk for one hour at 4℃. Primary antibodies against ERK, p-ERK, MEK, p-MEK, HRAS, Raf-1, Bax, Bcl-2 and Caspase-3 were diluted at a concentration of 1:500–1:1000 in blocking buffer. Membranes were then incubated with diluted primary antibodies overnight at 4°C, which was followed by incubation with secondary antibody for one hour at 37°C. After each membrane was washed three times with TBS containing 0.1% Tween-20 (TBST), it was treated with the DAB Substrate kit (Beyotime Biotechnology, Shanghai, China) and visualized using the Gel Image System. In order to compare the protein expression between untreated and treated cells with diosmin, data were normalized to loading control (β-actin) during densitometric analysis.

2.5. Statistical analysis

The results represent mean ± SD from at least three independent experiments. Data was analyzed using the SPSS 19.0 software. Only differences that were $P<0.01$ were considered statistically significant.

3. Results

3.1. Diosmin's targets to exert anti-cancer effect

The molecular structure of diosmin was obtained from the TCMSP platform (Fig. S1), and downloaded in the mol2 format. The diosmin structure consists of two phenolic hydroxyl groups and two monosaccharide molecules, which refers to a flavonoid glycoside compound. The molecular weight of diosmin is 608.60, and thus, it a small molecule substance. The autodock molecular docking software can be utilized to predict the interaction between the ligand diosmin and the receptor biological macromolecule.

The 300 potential activity targets of diosmin can be collected via the Pharmmapper database. In total, we obtained 27,228 targets related to anti-cancer effects. Using an intersection with the target of diosmin action from a previous analysis, 119 targets with fit value > 3 were chosen to analyze the intersection between the target proteins. After importing the obtained target proteins into the String database, and hiding the targets without interactions, the final 59 target proteins with interactions were obtained. The information is listed in Table 1.

3.2. Construction and analysis of protein interaction network

The cytoscape 3.6.1 software was used to construct the resulting interaction network diagram between target proteins (Fig. 2). The nodes in the figure represent related proteins, while the lines represent correlation between proteins. The larger the degree value, the larger the node, and the more importance it occupies within the entire network.

According to the data, the nodes with degree value>5.02, betweenness centrality>0.0354 and closeness centrality>0.3424 were chosen as the main nodes for subsequent analysis. Using the Disgenet database to search properties of the main node proteins, and the results are listed in Table 2. The data demonstrates that the anti-cancer process of diosmin largely involves a variety of enzymes (mitogen-activated protein kinase 1, superoxide dismutase 2, cyclin dependent kinase 2, dihydrofolate reductase), enzyme modulators, and interleukins 2.

3.3. Gene function and pathway analysis

After inputting the 13 important target proteins that were obtained from previous analysis into the shared data platform (https://david.ncifcrf.gov/) (DAVID Bioinformatics Resources 6.8) and setting the species as *homo sapiens*, GeneOntology (GO) analysis and Kyoto Encyclopedia of Genes and Genomes (KEGG) Path analysis was conducted.

GO analysis includes three parts, comprising of cellular component (CC), molecular function (MF) and biological process (BP). Overall, we obtained 35 items from the GO analysis, and 23 items had a corrected P value of less than 0.05. Among them, there are four CC items, which mainly involved the cytosol, nucleoplasm, extracellular exosome, and caveola. In addition, there was 1 MF item (ATP binding). There are also 18 BP items, which were found to be mainly related to positive regulation of cell proliferation, positive regulation of cell migration, MAPK cascade, and cellular response to insulin stimulus (Fig. 4A; Table 3). After filtering for corrected P value less than 0.05, the KEGG pathway analysis obtained a total of 14 items (Fig. 4B; Table 4). These included metabolic pathways with seven targets involved, PI3K-Akt signaling pathways with five targets involved, FoxO signaling pathway with five targets involved, insulin signaling pathway with four targets involved, purine metabolism pathway with four targets involved and other signaling pathways closely related to the anti-tumor effects of diosmin. By drawing the interaction network diagram of the first three main pathways (Fig. S2), we can see that the MAPK signaling pathway is closely related to these three pathways, so it has become the most focused pathway.

3.4. The molecular docking

Go and KEGG pathway analysis results indicated that frequency of MAPK1 and HRAS involved in gene function and biological pathways topped the list (17 and 19), followed by INSR (13), GCK (13) and CDK2 (10). Therefore, we performed the optimum docking conformation of MAPK1, HRAS, INSR, GCK, CDK2 and diosmin using the AutoDock with Lamarckian Genetic Algorithm, respectively. The results demonstrated that the binding energy of these five protein molecules with diosmin are -4.97, -4.85, -6.36, -6.74 and -4.17 kcal/mol by forming H-bond with multiple binding sites (Table 5, Fig. 4).

3.5. Effect of diosmin on cell inhibition

Starting from a concentration of 150 μg/mL, diosmin exhibited inhibition on HepG2 cells in a concentration-dependent manner, with a significant effect at 200~400 μg/mL ($P<0.01$; Fig. 5A). Accordingly, we further examined the mechanical behavior of 200 μg/mL diosmin using morphological observation. H&E staining showed that the internal structure of the treatment group was disordered with the condensed and aggregated chromatin, ruptured cell membrane and blue-violet particles, which appeared inside the treatment group (Fig. 5B). Then, the cell membrane stretched into an irregular shape, the cell swelling ruptured, and produced vesicles. In addition, diosmin attenuated proliferative activity by reducing the size and number of colonies compared to the untreated controls in HepG2 by colony formation assay (Fig. 5C).

We measured expression of the main proteins of MAPK signaling pathway, RAS/Raf1/MEK/ERK obtained from the previous network pharmacological analysis. Compared to the untreated cells, we observed 0.64-fold, 0.42-fold, 0.45-fold and 0.31-fold decrease in protein expression level in cells that were treated with 200 μg/mL of diosmin for p-ERK, p-MEK, HRAS and Bcl-2, respectively. There were 16.09-fold and 5.24-fold increase for Bax/Bcl-2 ratio and Caspase-3 expression. These differences were statistically significant ($P<0.01$) (Fig. 5D). Furthermore, protein levels of Raf-1 were found to be increased by 1.05-fold in treated cells, though difference was not statistically significant (Fig. 5D).

4. Discussion

Studies have reported that diosmin has an inhibitory effect on the proliferation of a variety of cancer cells. Dung *et al.* discovered that diosmin was able to inhibit the viability of the liver cancer cell line HA22T in a dose-dependent manner and significantly reduces the expression of related proteins to improve cell growth by activating the p53 protein and PI3K-Akt-MDM2 signaling pathway [23, 24]. Rajasekar *et al.* indicated that diosmin inhibits the phosphorylation of JAK-1 caused by an increase of IL-6, and the later phosphorylation of STAT-3, which makes the Bax/Bcl-2 ratio imbalance and triggers its downstream Caspase cascade reaction to induce cell apoptosis [25]. Buddhan *et al.* identified that diosmin may be able to down-regulate the expression of Bcl-2 in the skin cancer cell line A431 and inhibit cell invasion [26]. Perumal *et al.* disclosed that diosmin had a beneficial therapeutic effect on N-nitrosodiethylamine (NDEA)-induced liver cancer in adult Wistar rats by down-regulating the anti-apoptotic protein Bcl-2 and up-regulating the pro-apoptotic protein Bax [27]. However, only the effect on HepG2 cells is rarely reported, and there is no hints about the signaling pathway of action. The liver cancer has become the sixth most common cancer and the second leading cause of cancer deaths worldwide, so this study was conducted to study the effect of Diosmin on the proliferation of HepG2 cells. The results showed that diosmin over 150 μg/mL could inhibit proliferation. Moreover, compared with the blank group, the Diosmin-treated group not only destroyed cell morphology, but also significantly reduced the clone numbers of cancer cells.

In order to explore the possible pathway of action, we performed network pharmacological analysis. The related pathways of diosmin's tumor suppressor effect were mainly PI3k-Akt signaling pathway, FoxO signaling pathway, and insulin signaling pathway, according to P value from the KEGG pathway analysis,. Interaction network diagram showed MAPK signaling pathway was closely related to these three pathways. The MAPK signaling pathway has been reported in some studies as an effector on other types of cancer cells. Jiang *et al.* discovered that C-phycocyanin was able to induce MDA-MB-231 cell apoptosis through the MAPK signaling pathways [28]. Yang *et al.* indicated that Morusin inhibited cell growth and migration by down-regulating the ERK phosphorylation level proteins [29]. Yang *et al.* found that Fangchinoline derivatives induced cell cycle arrest and apoptosis in human leukemia cell lines via suppression of PI3K/AKT and MAPK signaling pathway [30].

The MAPK pathway consists of different signaling cascades, of which the Ras–Raf–MAPK/ERK kinase is one of the most dysregulated in human cancer. RAS is a small GTPase whose active form is combined with downstream effector molecules, including Raf and PI3K, in order to promote cell growth and proliferation. The acceleration of RAS signaling can cause tumorigenesis, invasion and metastasis of different cancers. In the T24 bladder cancer (BC) cell line in 1982, HRAS was the first human oncogene to be reported, as it was found to be mutated or up-regulated across a variety of cancers [31]. Therefore, in order to verify the important role of MAPK pathway in diosmin inhibiting the proliferation of HepG2 cells, we detected the expression of main proteins involved in the MAPK signaling pathway, HRAS, Raf1, MEK and ERK. Expression of p-ERK, p-MEK and HRAS down-regulated significantly. Meanwhile, activated MAPK pathway up-regulated downstream multi-effect molecules Bax and Caspase-3 and down-regulated Bcl-2, thereby cause the apoptosis of HepG2 cells. Consequently, the RAS-MAPK signaling pathway was indeed an innegligible pathway for diosmin to exert its anti-tumor effect in HepG2 cells.

5. Conclusion

Herein, network pharmacology analysis demonstrated that the antitumor effect of diosmin comprised a comprehensive effect of multi-cell signaling pathway, multi-biological process and multi-target. *In vitro* experiments identified that diosmin exerts anti-cancer effects on HepG2 cells. Comprehensive analysis reveals that diosmin has an anti-cancer role most probably by MAPK signaling pathway. Cell experiments has verified diosmin inhibits transcription by decreasing phosphorylating level of ERK and MEK and promote apoptosis by increasing expression ratio of Bax/Bcl-2 and Caspase-3 (Fig. 6).

Declarations

Conflict of interest

The authors declare no conflict of interest exists.

Ethical approval

This article does not contain any studies with human participants or animals performed by any of the authors.

Data Availability Statement

The authors declare that the data supporting the findings of this study are available within the article and its supplementary information files.

Funding

This study was supported by Chunhui Project of the Ministry of Education, China (grant number HLJ2019005).

Contributions

Rongchun Wang and Weihong Lu designed the experiments. Cuilin Cheng carried out experiments and wrote the manuscript. Debin Xia and Yingchun Zhang analyzed experimental results. Ning Xu collected and reorganized the data. Zhiqiang Zheng commented on previous versions of the manuscript. All authors read and approved the final manuscript.

Acknowledgements

We gratefully acknowledge MogoEdit for offering quality editing services.

References

1. Wan G, Gao F, Chen J, et al (2017) Nomogram prediction of individual prognosis of patients with hepatocellular carcinoma. BMC Cancer 17:91–101. https://doi.org/10.1186/s12885-017-3062-6
2. Gheena S, Ezhilarasan D (2019) Syringic acid triggers reactive oxygen species–mediated cytotoxicity in HepG2 cells. Hum Exp Toxicol 38:694–702. https://doi.org/10.1177/0960327119839173
3. Zhong JH, Wu FX, Li H (2014) Hepatic resection associated with good survival for selected patients with multinodular hepatocellular carcinoma. Tumor Biol 35:8355–8358. https://doi.org/10.1007/s13277-014-2571-z
4. Fang Y, Yang W, Cheng L, et al (2017) EGFR-targeted multifunctional polymersomal doxorubicin induces selective and potent suppression of orthotopic human liver cancer in vivo. Acta Biomater 64:323–333. https://doi.org/10.1016/j.actbio.2017.10.013
5. Cao MR, Li Q, Liu ZL, et al (2011) Harmine induces apoptosis in HepG2 cells via mitochondrial signaling pathway. Hepatobiliary Pancreat Dis Int 10:599–604. https://doi.org/10.1016/S1499-3872(11)60102-1
6. Meyer T (2018) Treatment of advanced hepatocellular carcinoma: beyond sorafenib. lancet Gastroenterol & Hepatol 3:218–220. https://doi.org/10.1016/s2468-1253(17)30255-8

7. Bartek J, Lukas C, Lukas J (2004) Checking on DNA damage in S phase. Nat Rev Mol Cell Biol 5:792–804. https://doi.org/10.1038/nrm1493
8. He N, Tian L, Zhai X, et al (2018) Composition characterization, antioxidant capacities and anti-proliferative effects of the polysaccharides isolated from Trametes lactinea (Berk.) Pat. Int J Biol Macromol 115:114–123. https://doi.org/10.1016/j.ijbiomac.2018.04.049
9. Romagnolo DF, Selmin OI (2012) Flavonoids and Cancer Prevention: A Review of the Evidence. J Nutr Gerontol Geriatr 31:206–238. https://doi.org/10.1080/21551197.2012.702534
10. Aggarwal BB, Shishodia S (2006) Molecular targets of dietary agents for prevention and therapy of cancer. Biochem Pharmacol 71:1397–1421. https://doi.org/10.1016/j.bcp.2006.02.009
11. Pick A, Müller H, Mayer R, et al (2011) Structure-activity relationships of flavonoids as inhibitors of breast cancer resistance protein (BCRP). Bioorganic Med Chem 19:2090–2102. https://doi.org/10.1016/j.bmc.2010.12.043
12. Nijveldt RJ, Van Nood E, Van Hoorn DEC, et al (2001) Flavonoids: A review of probable mechanisms of action and potential applications. Am J Clin Nutr 74:418–425. https://doi.org/10.1093/ajcn/74.4.418
13. Szeleszczuk Ł, Pisklak DM, Zielińska-Pisklak M, Wawer I (2017) Spectroscopic and structural studies of the diosmin monohydrate and anhydrous diosmin. Int J Pharm 529:193–199. https://doi.org/10.1016/j.ijpharm.2017.06.078
14. Patel K, Gadewar M, Tahilyani V, Patel DK (2013) A review on pharmacological and analytical aspects of diosmetin: A concise report. Chin J Integr Med 19:792–800. https://doi.org/10.1007/s11655-013-1595-3
15. Lewinska A, Adamczyk-Grochala J, Kwasniewicz E, et al (2017) Diosmin-induced senescence, apoptosis and autophagy in breast cancer cells of different p53 status and ERK activity. Toxicol Lett 265:117–130. https://doi.org/10.1016/j.toxlet.2016.11.018
16. Al-Sheddi ES, Farshori NN, Al-Oqail MM, et al (2015) Portulaca oleracea seed oil exerts cytotoxic effects on human liver cancer (HepG2) and human lung cancer (A-549) cell lines. Asian Pacific J Cancer Prev 16:3383–3387. https://doi.org/10.7314/APJCP.2015.16.8.3383
17. Browning AM, Walle UK, Walle T (2005) Flavonoid glycosides inhibit oral cancer cell proliferation - role of cellular uptake and hydrolysis to the aglycones. J Pharm Pharmacol 57:1037–1041. https://doi.org/10.1211/0022357056514
18. Wang Y, Hu B, Feng S, et al (2020) Target recognition and network pharmacology for revealing anti-diabetes mechanisms of natural product. J Comput Sci 45:101186. https://doi.org/10.1016/j.jocs.2020.101186
19. Sriramulu DK, Wu S, Lee SG (2020) Effect of ligand torsion number on the AutoDock mediated prediction of protein-ligand binding affinity. J Ind Eng Chem 83:359–365. https://doi.org/10.1016/j.jiec.2019.12.009
20. Piñero J, Ramírez-Anguita JM, Saüch-Pitarch J, et al (2020) The DisGeNET knowledge platform for disease genomics: 2019 update. Nucleic Acids Res 48:D845–D855.

https://doi.org/10.1093/nar/gkz1021

21. Tiloke C, Phulukdaree A, Gengan RM, Chuturgoon AA (2019) Moringa oleifera Aqueous Leaf Extract Induces Cell-Cycle Arrest and Apoptosis in Human Liver Hepatocellular Carcinoma Cells. Nutr Cancer 71:1165–1174. https://doi.org/10.1080/01635581.2019.1597136
22. Da Silva TC, Cogliati B, Latorre AO, et al (2015) Pfaffosidic fraction from Hebanthe paniculata induces cell cycle arrest and caspase-3-induced apoptosis in HepG2 cells. Evidence-based Complement Altern Med 2015:9. https://doi.org/10.1155/2015/835796
23. Dung TD, Day CH, Binh TV, et al (2012) PP2A mediates diosmin p53 activation to block HA22T cell proliferation and tumor growth in xenografted nude mice through PI3K-Akt-MDM2 signaling suppression. Food Chem Toxicol 50:1802–1810. https://doi.org/10.1016/j.fct.2012.01.021
24. Dung TD, Lin CH, Binh TV, et al (2012) Diosmin induces cell apoptosis through protein phosphatase 2A activation in HA22T human hepatocellular carcinoma cells and blocks tumour growth in xenografted nude mice. Food Chem 132:2065–2073. https://doi.org/10.1016/j.foodchem.2011.11.149
25. Rajasekar M, Suresh K, Sivakumar K (2016) Diosmin induce apoptosis through modulation of STAT-3 signaling in 7,12 dimethylbenz(a)anthracene induced harmster buccal pouch carcinogenesis. Biomed Pharmacother 83:1064–1070. https://doi.org/10.1016/j.biopha.2016.08.019
26. Buddhan R, Manoharan S (2017) Diosmin reduces cell viability of A431 skin cancer cells through apoptotic induction. J Cancer Res Ther 13:471–476. https://doi.org/10.4103/0973-1482.183213
27. Perumal S, Langeshwaran K, Selvaraj J, et al (2018) Effect of diosmin on apoptotic signaling molecules in N-nitrosodiethylamine-induced hepatocellular carcinoma in experimental rats. Mol Cell Biochem 449:27–37. https://doi.org/10.1007/s11010-018-3339-3
28. Jiang L, Wang Y, Liu G, et al (2018) C-Phycocyanin exerts anti-cancer effects via the MAPK signaling pathway in MDA-MB-231 cells. Cancer Cell Int 1–14. https://doi.org/10.1186/s12935-018-0511-5
29. Yang C, Luo J, Luo X, et al (2020) Morusin exerts anti-cancer activity in renal cell carcinoma by disturbing MAPK signaling pathways. Ann Transl Med 8:. https://doi.org/10.21037/atm.2020.02.107
30. Yang J, Hu S, Wang C, et al (2019) Fangchinoline derivatives induce cell cycle arrest and apoptosis in human leukemia cell lines via suppression of the PI3K/AKT and MAPK signaling pathway. Eur J Med Chem 111898. https://doi.org/10.1016/j.ejmech.2019.111898
31. Satoshi S, Yoshino H, Miyamoto K, et al (2018) Targeting HRAS as a potential therapeutic target through RAS inhibitor salirasib in bladder cancer. Eur Urol Suppl 17:e655. https://doi.org/10.1016/s1569-9056(18)31294-6

Tables

Table 1 The anti-cancer targets of diosmin.

No.	Uniprot	Gene symbol	Fit	No.	Uniprot	Genesymbol	Fit
1	G6PI_HUMAN	*GPI*	3.593	31	P19623	*SRM*	3.554
2	P07741	*APRT*	3.572	32	P10827	*THRA*	3.585
3	PUR9_HUMAN	*ATIC*	4.66	33	FABP6_HUMAN	*FABP6*	3.595
4	JAK3_HUMAN	*JAK3*	3.691	34	TPIS_HUMAN	*TPI1*	3.813
5	RASH_HUMAN	*HRAS*	4.369	35	IMPA1_HUMAN	*IMPA1*	4.771
6	DYR_HUMAN	*DHFR*	3.64	36	AK1C2_HUMAN	*AKR1C2*	3.79
7	HDAC8_HUMAN	*HDAC8*	3.544	37	CDD_HUMAN	*CDA*	3.647
8	P24941	*CDK2*	3.581	38	MMP7_HUMAN	*MMP7*	3.562
9	STAT1_HUMAN	*STAT1*	3.794	39	A1AT_HUMAN	*SERPINA1*	3.74
10	HXK1_HUMAN	*HK1*	3.639	40	KTHY_HUMAN	*DTYMK*	3.569
11	P46926	*GNPDA1*	4.09	41	DPP4_HUMAN	*DPP4*	3.572
12	PDPK1_HUMAN	*PDPK1*	3.651	42	P14061	*HSD17B1*	3.614
13	IL2_HUMAN	*IL2*	3.525	43	INSR_HUMAN	*INSR*	3.796
14	IMDH1_HUMAN	*IMPDH1*	3.609	44	P28845	*HSD11B1*	3.761
15	P03956	*MMP1*	3.747	45	EPHA2_HUMAN	*EPHA2*	3.54
16	P08107	*HSPA1A*	3.718	46	CBR1_HUMAN	*CBR1*	3.771
17	Q9HAN9	*NMNAT1*	3.566	47	P04745	*AMY1A*	3.778
18	KPCT_HUMAN	*PRKCQ*	3.532	48	CP2C9_HUMAN	*CYP2C9*	3.676
19	ZAP70_HUMAN	*ZAP70*	3.832	49	P11586	*MTHFD1*	3.657
20	SHBG_HUMAN	*SHBG*	3.659	50	MK01_HUMAN	*MAPK1*	3.707
21	P10828	*THRB*	3.618	51	Q92831	*KAT2B*	5.027
22	P07686	*HEXB*	4.592	52	HXK4_HUMAN	*GCK*	3.988
23	ADK_HUMAN	*ADK*	4.171	53	CDK6_HUMAN	*CDK6*	4.173
24	CDC42_HUMAN	*CDC42*	3.781	54	LEG3_HUMAN	*LGALS3*	3.973
25	P04179	*SOD2*	3.517	55	BST1_HUMAN	*BST1*	3.888
26	NR1I2_HUMAN	*NR1I2*	3.979	56	TPH1_HUMAN	*TPH1*	4.111
27	CCL5_HUMAN	*CCL5*	3.529	57	Q06520	*SULT2A1*	3.606
28	B3GA1_HUMAN	*B3GAT1*	3.638	58	HINT1_HUMAN	*HINT1*	3.874

29	DHSO_HUMAN	*SORD*	3.88	59	ARGI2_HUMAN	*ARG2*	3.545
30	P35558	*PCK1*	4.227				

Table 2 The information of main protein nodes.

No.	Gene symbol	Full name	Protein class	Degree	Betweenness Centrality	Closeness Centrality
1	*DHFR*	Dihydrofolate reductase	Enzyme	13	0.2747	0.4754
2	*HRAS*	HRas proto-oncogene	Enzyme modulator	16	0.2070	0.4715
3	*MAPK1*	Mitogen-activated protein kinase 1	Kinase	15	0.1888	0.4603
4	*CDK2*	Cyclin dependent kinase 2	Kinase	8	0.1752	0.4496
5	*TPI1*	Triosephosphate isomerase 1	Enzyme	15	0.1162	0.4203
6	*INSR*	Insulin receptor	Kinase	7	0.0563	0.4203
7	*ATIC*	5-aminoimidazole-4-carboxamide ribonucleotide formyltransferase /IMP cyclohydrolase	Enzyme	9	0.0365	0.4113
8	*APRT*	Adenine phosphoribosyltransferase	none	9	0.1052	0.4056
9	*ADK*	Adenosine kinase	Kinase	9	0.0379	0.4056
10	*SOD2*	Superoxide dismutase 2	Enzyme	8	0.0454	0.4028
11	*IMPDH1*	Inosine monophosphate dehydrogenase 1	Enzyme	7	0.1218	0.3973
12	*GCK*	Glucokinase	Kinase	7	0.0383	0.3742
13	*IL2*	Interleukin 2	none	9	0.0498	0.3718

Table 3 Target proteins involved in GO analysis (P<0.05).

	Terms	Genes involved	P value
BP	positive regulation of cell proliferation	INSR, CDK2, MAPK1, HRAS, IL2	2.43E-4
	cellular response to insulin stimulus	INSR, GCK, APRT	1.33E-3
	AMP salvage	ADK, APRT	1.43E-3
	dihydrofolate metabolic process	DHFR, ATIC	2.14E-3
	tetrahydrofolate biosynthetic process	DHFR, ATIC	0.43E-3
	positive regulation of cell migration	INSR, MAPK1, HRAS	0.73E-3
	purine ribonucleoside monophosphate biosynthetic process	ATIC, IMPDH1	0. 93E-3
	purine-containing compound salvage	ADK, APRT	1.00E-3
	positive regulation of glycogen biosynthetic process	INSR, GCK	0.011
	nucleoside metabolic process	ATIC, APRT	0.013
	MAPK cascade	MAPK1, HRAS, IL2	0.014
	carbohydrate phosphorylation	ADK, GCK	0.016
	canonical glycolysis	TPI1, GCK	0.019
	glycolytic process	TPI1, GCK	0.024
	positive regulation of DNA replication	INSR, HRAS	0.030
	positive regulation of nitric oxide biosynthetic process	INSR, SOD2	0.030
	positive regulation of interferon-gamma production	HRAS, IL2	0.032
	Ras protein signal transduction	CDK2, HRAS	0.049
CC	cytosol	DHFR, ATIC, TPI1, IMPDH1, CDK2, ADK, MAPK1, HRAS, GCK, APRT	2.79E-5
	nucleoplasm	DHFR, IMPDH1, CDK2, ADK, MAPK1, GCK, APRT	0.51E-3
	extracellular exosome	ATIC, TPI1, INSR, MAPK1, SOD2, APRT	0.027

	caveola	INSR, MAPK1	0.042
MF	ATP binding	INSR, CDK2, ADK, MAPK1, GCK	0.0170

Table 4 Target proteins involved in KEGG analysis (P<0.05).

Pathway	Gene involved	P value
Metabolic pathways	DHFR, ATIC, TPI1, IMPDH1, ADK, GCK, APRT	0.011
FoxO signaling pathway	HRAS, INSR, CDK2, MAPK1, SOD2	6.04E-5
PI3K-Akt signaling pathway	HRAS, INSR, CDK2, MAPK1, IL2	0.002
Insulin signaling pathway	HRAS, INSR, MAPK1, GCK	0.002
Purine metabolism	ATIC, IMPDH1, ADK, APRT	0.003
Type II diabetes mellitus	INSR, MAPK1, GCK	0.003
Central carbon metabolism in cancer	HRAS, MAPK1, GCK	0.005
Prolactin signaling pathway	HRAS, MAPK1, GCK	0.006
Prostate cancer	HRAS, CDK2, MAPK1	0.010
T cell receptor signaling pathway	HRAS, MAPK1, IL2	0.013
Hepatitis B	HRAS, CDK2, MAPK1	0.025
Viral carcinogenesis	HRAS, CDK2, MAPK1	0.048

Table 5 AutoDock binding energy values and H-bond forming residues of the lead molecules.

Protein	Binding energy (kcal/mol)	Binding sites
MAPK1	-4.97	ASN-85, LYS-117, SER-17, TYR-32, ASP-30
HRAS	-4.85	ASN-281, LEU-222, LEU-121
INSR	-6.36	ARG-1128, GLU-1135, GLU-1142, PHE-1171
CDK2	-6.74	HIS-84, ASP-92, ASP-86, LYS-88, ASP-145
GCK	-4.17	GLU-17, GLN-24, PHE-23, LEU-25, GLN-26, HIS-380, GLU-27

Figures

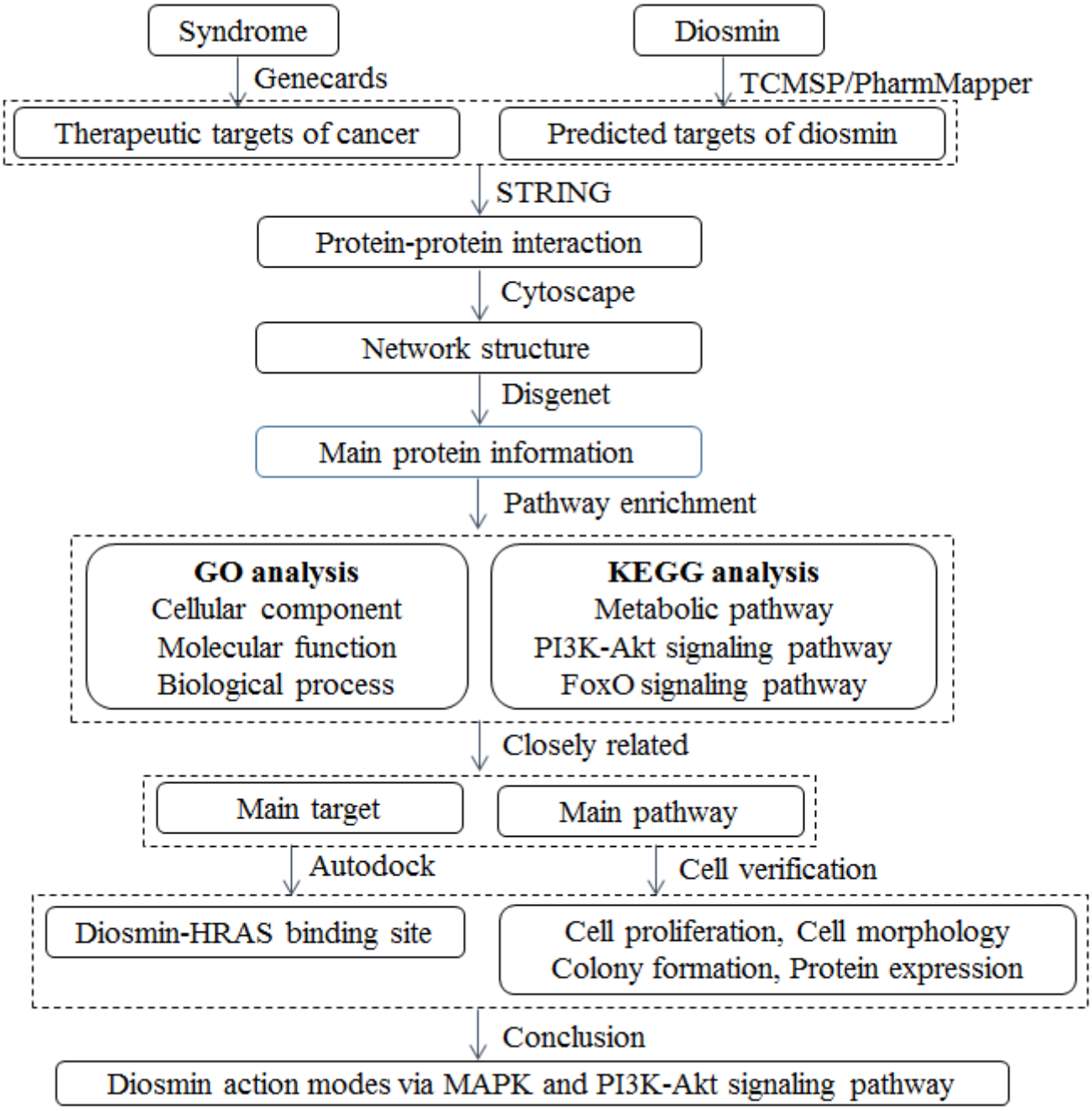

Figure 1

The flowchart of network pharmacology-based strategy for the anti-cancer effect of diosmin. Firstly, the potential target proteins of diosmin were analyzed and identified using Network Pharmacology. Next, molecular docking analysis was carried out to determine the site of action of the main target proteins using the small molecule diosmin as a substrate. Finally, cellular inhibition assays were designed and performed using HepG2 cells in order to explore anti-cancer effects and mechanisms of diosmin.

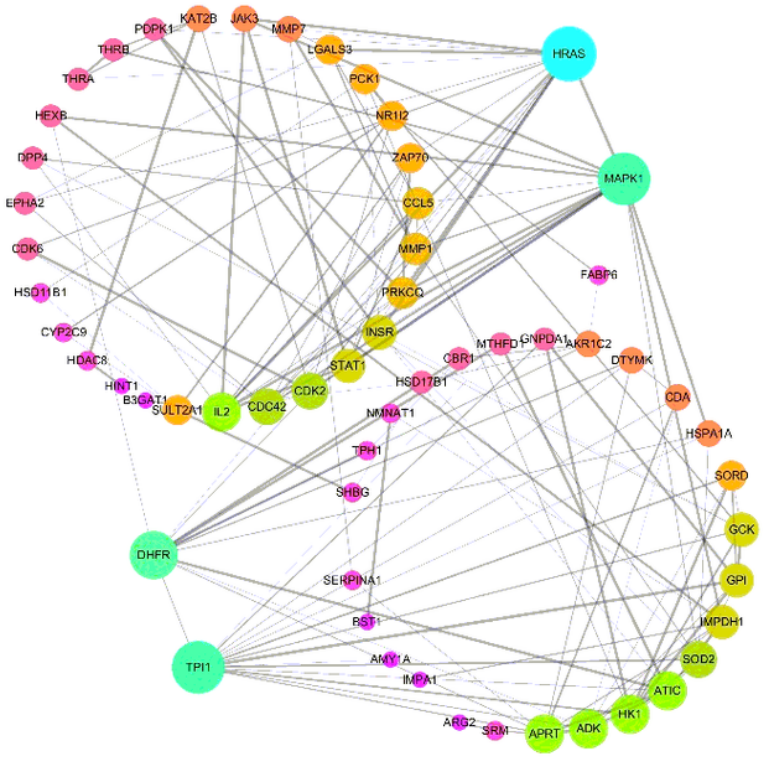

Figure 2

The protein-protein interaction network. The nodes within this figure represent related proteins, and the lines represent correlation between the proteins. The larger the degree value, the larger the node, and the more important it occupies within the entire network.

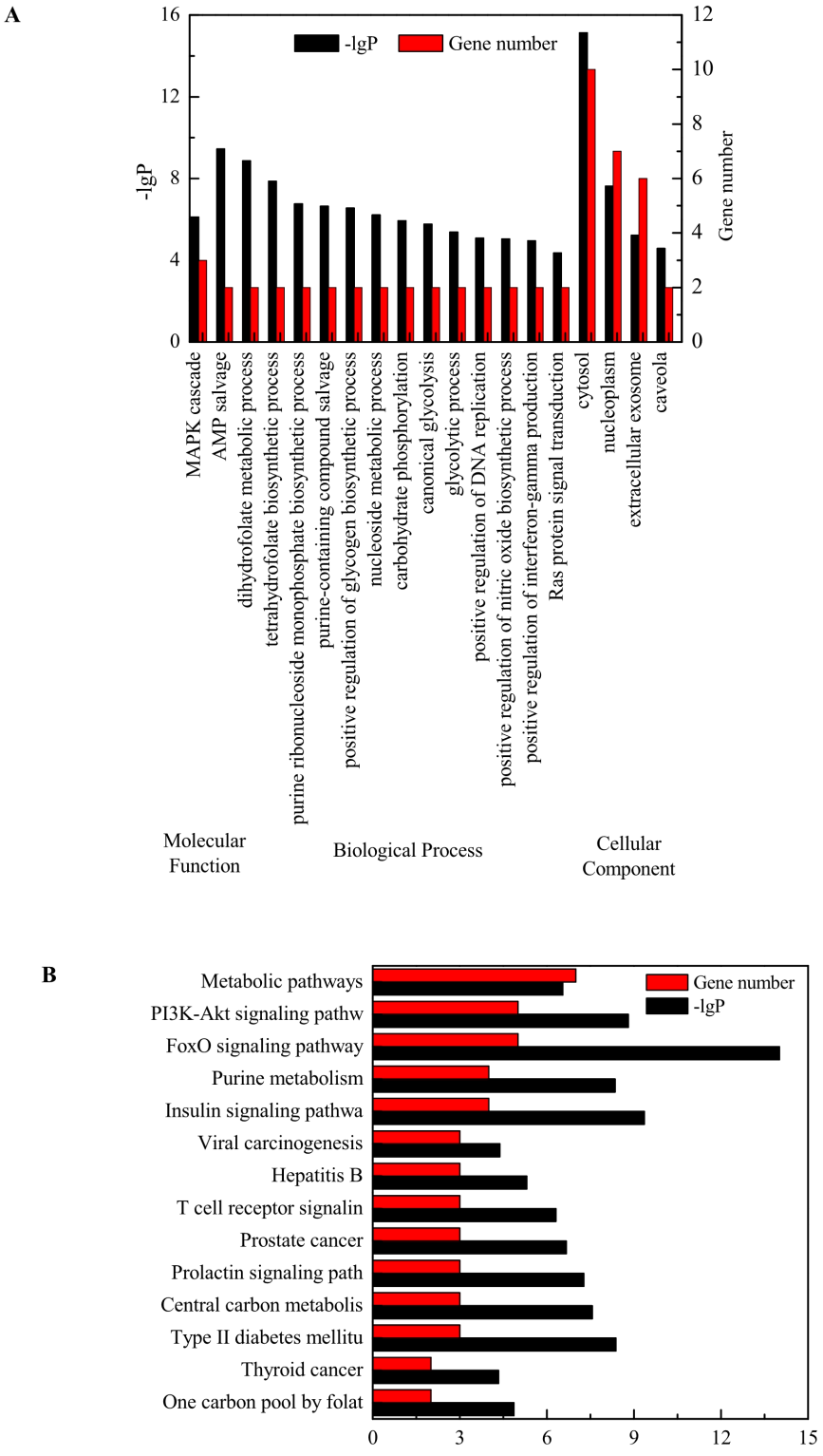

Figure 3

GO enrichment analysis (A) and KEGG enrichment analysis (B).

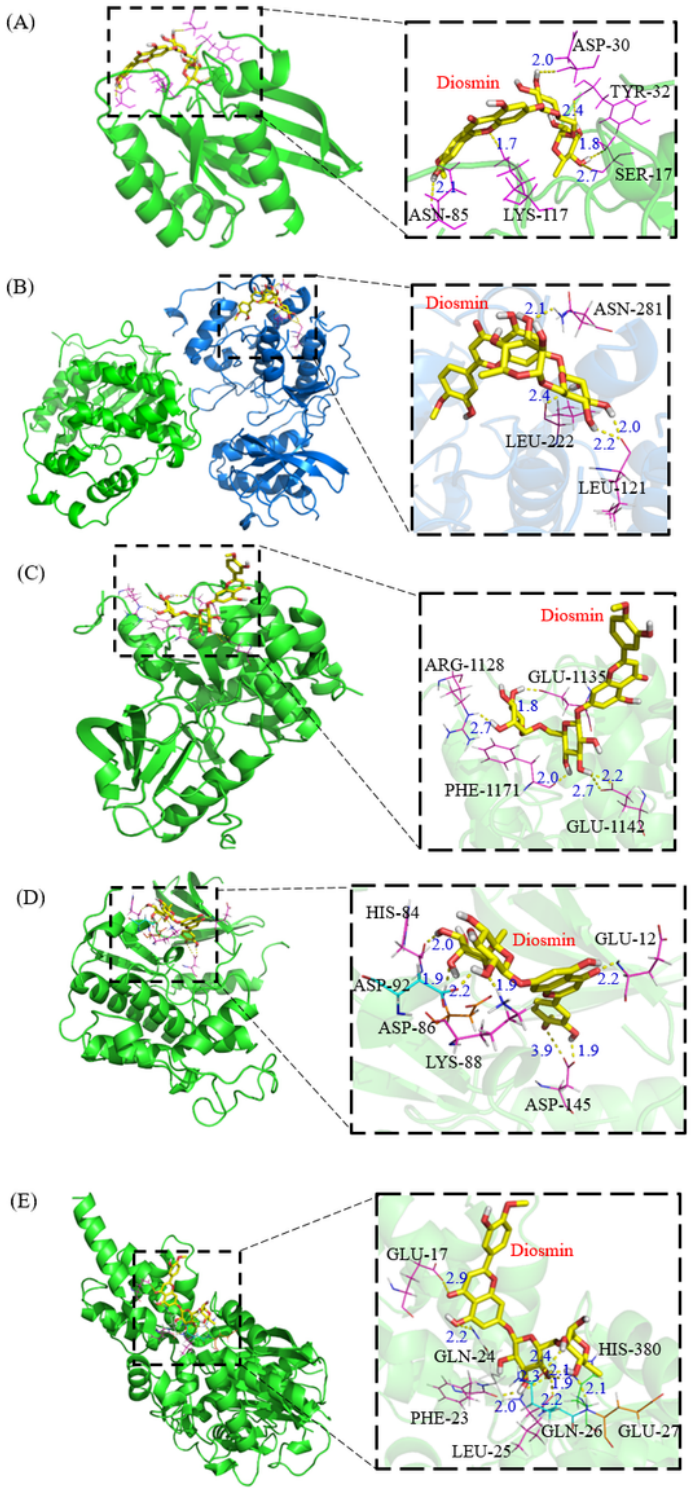

Figure 4

Molecular docking mode of diosmin with HRas (A), MAPK1 (B), INSR (C), CDK2 (D) and GCK (E).

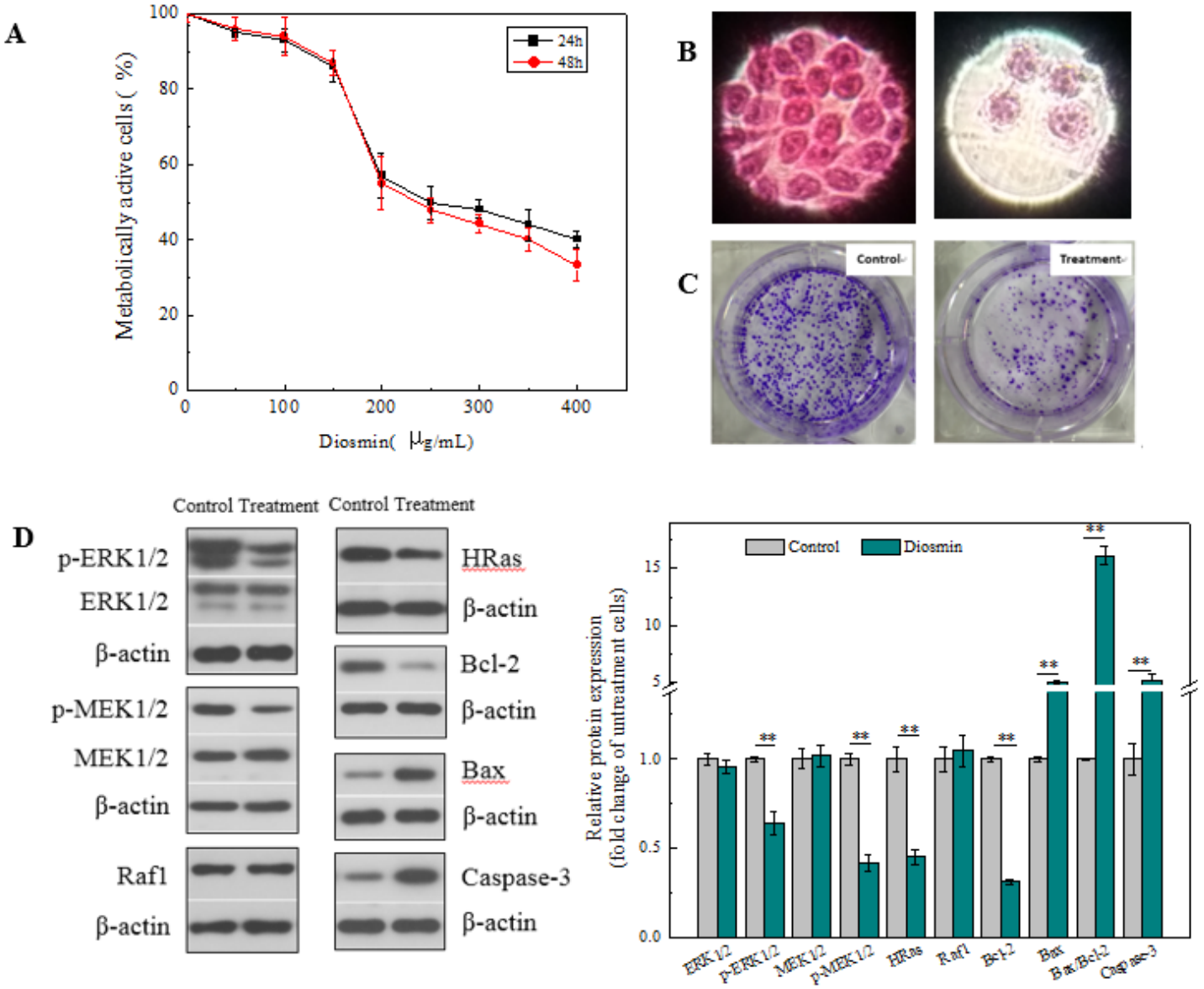

Figure 5

Cytotoxic and antiproliferative effects of diosmin on HepG2 cells. (A) Cytotoxicity of diosmin in HepG2 cell line. The cells were treated with various concentration of diosmin for 24 h and 48 h. Cell viability was determine using the MTT assay. (B) HepG2 cells were treated with 200 μg/mL diosmin for 24 h and then their morphology was observed under an inverted microscope (Life technologies brand) (HE; magnification×100). (C) Colony formation assay. HepG2 cells were treated with 200 μg/mL of diosmin. Culture media was changed every three days. Cells were incubated for two weeks to grow colonies at 37°C under conditions of 5% CO2, fixed with methanol, stained with crystal violet solution and dried overnight. The wells were detected using a camera. (D) Western blot analysis of key proteins in HepG2 cells after 24 h treatment or untreated with 200 μg/mL diosmin. Data were normalized to β-actin.

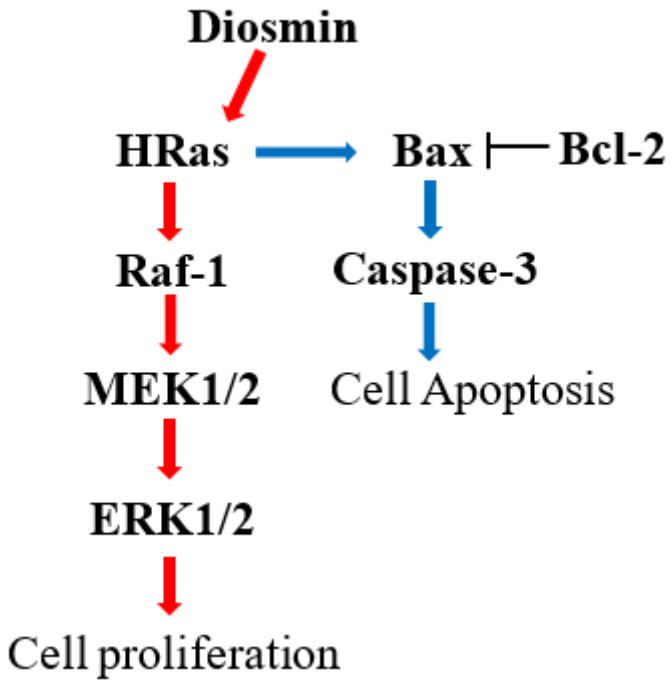

Figure 6

Schematic diagram of diosmin action modes via MAPK signaling pathway.

Supplementary Files

This is a list of supplementary files associated with this preprint. Click to download.

- SuppFig.docx
- data.xlsx